

CREATION OF SUPER-RESOLUTION NON-DIFFRACTION BEAM BY MODULATING CIRCULARLY POLARIZED LIGHT WITH TERNARY OPTICAL ELEMENT

Jingsong Wei^{1, *}, Yikun Zha^{1, 2}, and Fuxi Gan¹

¹Shanghai Institute of Optics and Fine Mechanics, Chinese Academy of Sciences, Shanghai 201800, China

²University of Chinese Academy of Sciences, Beijing 100049, China

Abstract—In order to obtain a super-resolution non-diffraction beam, we propose a fast searching method to design a ternary optical element combined with the circularly polarized light. The optimized results show that a beam with a spot size of 0.356λ and depth of focus of 8.28λ can be achieved by focusing with an oil lens of numerical aperture $NA = 1.4$ and refractive index of oil $n = 1.5$. The analysis reveals that the spot size of transverse component is 0.273λ , indicating that the super-resolution effect mainly comes from the transverse component. The spot size inside the media can theoretically reach down to 0.273λ because the spot size inside the media is mainly determined by the transverse component.

1. INTRODUCTION

The goal to pursue the small spot in the field of optical data storage and photolithography has never stopped [1, 2]. In recent years, there are lots of studies on the small focusing spot. Among them, some researchers analyzed the focusing light to a tighter spot [3, 4] and focusing on properties of Maxwell's fish eye medium [5]. Some methods to obtain the small spot were also proposed, such as achieving a sharper focus by using radially polarized light beam [6] and optimizing the focusing of linearly polarized light [7, 8]. However, it is difficult to realize the spot below diffraction limit due to the optical diffraction limit effect. In order to break through the diffraction limit, lots of ways to obtain super-resolution non-diffraction beam were presented and discussed such as hyperlens and super-oscillatory lens [9–11],

Received 20 April 2013, Accepted 3 June 2013, Scheduled 26 June 2013

* Corresponding author: Jingsong Wei (weijingsong@siom.ac.cn).

utilizing superlens to turn evanescent waves into propagating waves and obtain subwavelength imaging [12, 13], handling of the evanescent waves with near field diffraction structures [2, 14], and super-resolution apodization through pupil masks [14–18]. In these methods, the super-resolution pupil filters (or phase plates) with amplitude and phase modulations are always hot subjects. Researchers used phase-only plate to modulate the incident light and adopted the phase plate with central block or annular beam without phase modulation. According to our experience, the super-resolution and depth of focus (DOF) extension effects are good for phase plate with central block, but the drawback is that much energy is blocked. In addition, most of them used radially polarized beam as incident light to conduct subsurface imaging, which is difficult to apply in optical data storage and photolithography due to the deterioration of resolution for a longitudinally polarized beam inside materials [2, 18]. To overcome this drawback, Grosjean et al. [1] proposed a type of material that is sensitive only to the longitudinal component. In the present work, based on the confinement of axial uniformity within a certain distance along the optical axis and the full width at half maximum (FWHM) in the focal plane, we propose a fast searching method to design a ternary optical element combined with a circularly polarized light to obtain a super-resolution non-diffraction beam. The proposed ternary optical element has three different amplitude transmissions $(-1, 0, 1)$. The optimized results show that a beam with a spot size of 0.356λ and DOF of 8.28λ can be obtained by focusing with an oil lens of numerical aperture $NA = 1.4$ and a refractive index of oil $n = 1.5$. Further analysis shows that the spot size of the transverse component is 0.273λ , indicating that the super-resolution effect comes mainly from the transverse component, and the longitudinal component increases the spot size. The longitudinal component has been known to decay rapidly when it passes through the media, hence the spot size inside the media is mainly determined by the transverse component. That is, the spot size inside the media can theoretically reach down to 0.273λ which is very useful for nano-optical information storage and nanolithography.

2. DESIGN METHOD AND PRINCIPLE

First, we analyze the dependence of the FWHM and DOF on the annulus ratio of the annular aperture illumination under the focusing condition with an oil lens of $NA = 1.4$ and refractive index of oil $n = 1.5$. The annulus ratio is defined as the inner radius divided by the outer radius. Then, we compare the dependence of the FWHM and

DOF for circular polarization illumination with the radial polarization illumination.

Figure 1(a) shows that the DOF for the circularly polarized light is almost the same as that of the radially polarized light when the annulus ratio is over 0.6. Figure 1(b) shows that the FWHM of the radial polarization is larger than the circular polarization when the annulus ratio is less than 0.7, and is smaller than the circular polarization when the annulus ratio is more than 0.7. Further analysis reveals that the FWHM of the longitudinal component of the radial polarization is smaller than the transverse component of the circular polarization when the annulus ratio is below 0.7, and continuously increasing the annulus ratio results in almost the same value of the two components. Thus, comparison with the radially polarized illumination indicates that, in practical applications, the circularly polarized illumination is also a good candidate for obtaining a small spot at an annulus ratio of over 0.7 if the materials are only sensitive to the transverse component.

Based on Figure 1, the proposed system configuration is shown in Figure 2. A circularly polarized beam strikes on the ternary optical element and is then focused by an oil lens with an NA of 1.4 and refractive index of oil $n = 1.5$. The ternary optical element is designed as a five-zone annular phase plate, and the configuration of each zone is shown in Figure 2(b), where the innermost central zone (marked in black) is blocked and has zero transmission and the other four belts have alternate transmissions of -1 and $+1$. The yellow color represents the -1 transmission, and the white color represents the $+1$ transmission. In the focal region of the lens, a super-resolution focal spot with an ultra-long DOF is obtained. The angle θ_i ($i = 1, 2, 3, 4$)

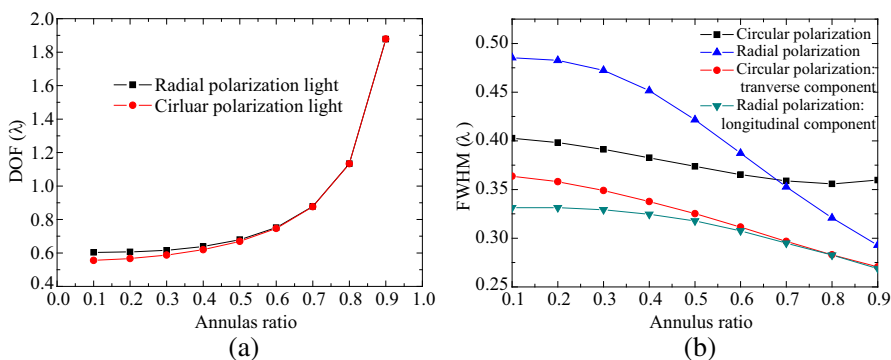


Figure 1. Dependence of the (a) DOF and (b) FWHM on the annulus ratio for the circular and radial polarization.

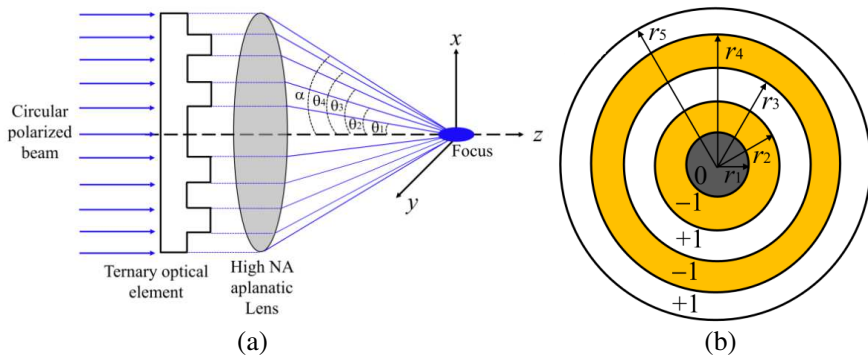


Figure 2. Schematic of the ternary optical element, (a) diagram of the focusing system, (b) configuration of the ternary optical element.

corresponds to the aperture half-angle of the i th belt and is computed as $\theta_i = \sin^{-1}(r_i \text{NA}/n)$, where r_i is the normalized radius of the i th belt.

According to the vector Debye integrals, the electric field in the vicinity of the focal region is expressed as [19]

$$\begin{aligned} e_x &= -iA[I_0 + I_2(\cos 2\varphi + i \sin 2\varphi)] \\ e_y &= -iA[iI_0 - iI_2(\cos 2\varphi + i \sin 2\varphi)], \\ e_z &= -2AI_1(\cos \varphi + i \sin \varphi) \end{aligned} \tag{1}$$

where φ is the azimuth angle. Constant $A = \pi l_0 f/\lambda$, where f is the focal length and l_0 the amplitude distribution of the incident field. The uniform amplitude plane wave is used as the incident light, thus l_0 is set to unity. λ is the wavelength of the incident light. The maximum aperture half angle is $\alpha = \sin^{-1}(\text{NA}/n)$. The wave number is $k = 2\pi n/\lambda$, where n is the refractive index of the oil. I_0 , I_1 , and I_2 are the integrals evaluated over the aperture half-angle α and are written as follows,

$$\begin{aligned} I_0 &= \int_0^\alpha t(\theta)\sqrt{\cos \theta} \sin \theta(1 + \cos \theta)J_0(kr \sin \theta) \exp(ikz \cos \theta)d\theta \\ I_1 &= \int_0^\alpha t(\theta)\sqrt{\cos \theta} \sin^2 \theta J_1(kr \sin \theta) \exp(ikz \cos \theta)d\theta \\ I_2 &= \int_0^\alpha t(\theta)\sqrt{\cos \theta} \sin \theta(1 - \cos \theta)J_2(kr \sin \theta) \exp(ikz \cos \theta)d\theta \end{aligned} \tag{2}$$

where θ is the aperture half-angle and $t(\theta)$ the transmission function of the ternary optical element, which is expressed as

$$t(\theta) = \begin{cases} 0, & \text{for } 0 \leq \theta < \theta_1, \\ -1, & \text{for } \theta_1 \leq \theta < \theta_2, \quad \theta_3 \leq \theta < \theta_4, \\ 1, & \text{for } \theta_2 \leq \theta < \theta_3, \quad \theta_4 \leq \theta < \alpha. \end{cases} \quad (3)$$

The radius of the i th zone is normalized to the outermost pupil radius of the five-zone annular ternary optical element, and $r_i = \sin \theta_i / \sin \alpha$. J_0 , J_1 , and J_2 are the zeroth, first, and second order Bessel functions of the first kind, respectively.

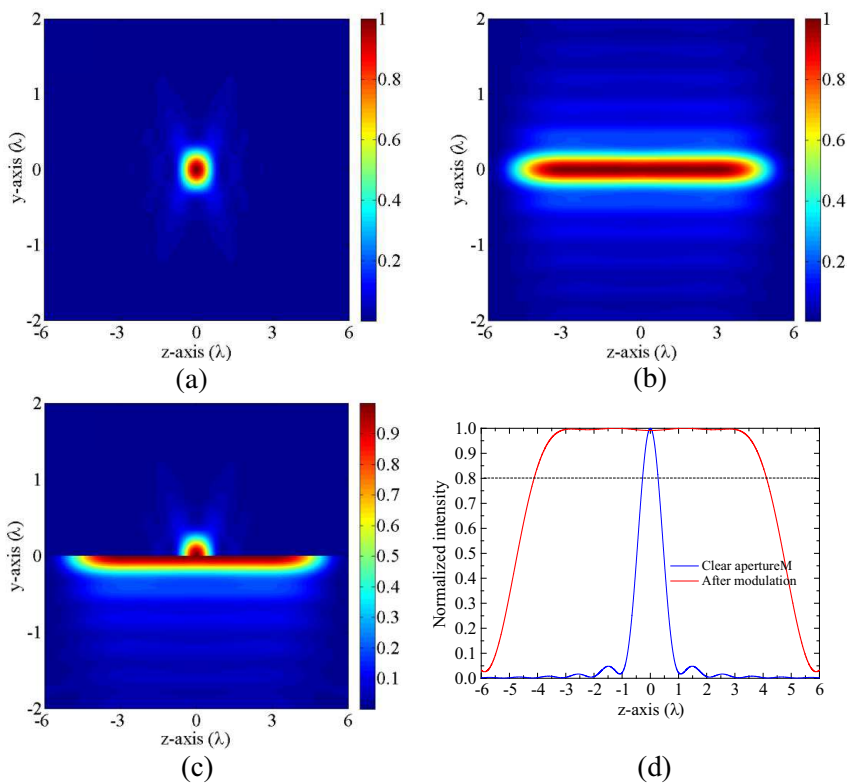


Figure 3. (Color Online) Electric energy density distributions on the y - z plane, (a) clear aperture and (b) modulated by the ternary optical element, (c) comparison between the upper half of (a) and lower half of (b), (d) electric energy density distribution along the z -axis of the clear aperture and that modulated by the ternary optical element.

3. THE DESIGN RESULTS AND ANALYSIS

The method that we use in designing the ternary optical element is the global search optimization (GSO) algorithm combined with two confinement requirements, which allow a fast search speed. One confinement requirement is the uniformity δ along the z -axis, defined as the ratio of the intensity difference to the summation of the maximum and minimum intensities in the range from -1.5λ to 1.5λ . The other is the FWHM of the focal spot. In our calculation, δ is set to below 0.05, and the FWHM was set smaller than 0.36λ . The search space was located in the range of the normalized radii (r_1, r_2, r_3, r_4) with a tolerance of $\Delta r = 0.01$. The starting point for r_1 was 0.5. Our computing environment was the Matlab R2012a UNIX, which runs on an eight-core parallel computing system. The optimization calculation time was 0.5879 h, which was much faster than the GSO algorithm based on different searching criteria. Then, the FWHM values were sorted from small to large, and some favorable results were selected. To obtain an ultra-long uniform subwavelength light beam, the two decimal digits of the tolerance can be easily extended manually to four decimal digits according to experience. Finally, some good results were obtained. The most important feature of our optimization method is the saving in time. Here, one of the optimized solutions was obtained as $r_1 = 0.8721$, $r_2 = 0.8869$, $r_3 = 0.9117$, $r_4 = 0.9864$, and $r_5 = 1$. Correspondingly, the electric energy density distributions on the y - z plane are shown in Figure 3. For comparison, the electric energy density distribution of the clear aperture is given in Figure 3(a). Figure 3(b) shows that the DOF is elongated by the ternary optical element. If we define DOF as the two-point distance where the maximum intensity I_{\max} along the z -axis decreases to $0.8I_{\max}$, then the DOF modulated by the ternary optical element is approximately 8.283λ , which is approximately 15 times larger than that generated by the clear aperture focusing. Compared with the clear aperture case shown in Figure 3(a) where the original beam has an FWHM of 0.4043λ and DOF of 0.552λ , the light beam modulated by the ternary optical element in our optimized design has an FWHM of 0.3562λ and DOF of 8.283λ , which means that the beam propagates without divergence over 8.283λ . Thus, the beam is a highly localized super-resolution non-diffraction beam.

One can note that the optimized radii are too precise, causing some difficulties in the fabrication of the ternary optical element. Therefore, the radii are approximated to three decimal digits, i.e., $r_1 = 0.873$, $r_2 = 0.887$, $r_3 = 0.913$, $r_4 = 0.988$, and $r_5 = 1$. We assume that the radius of ternary optical element is 2 mm, so the machining precision

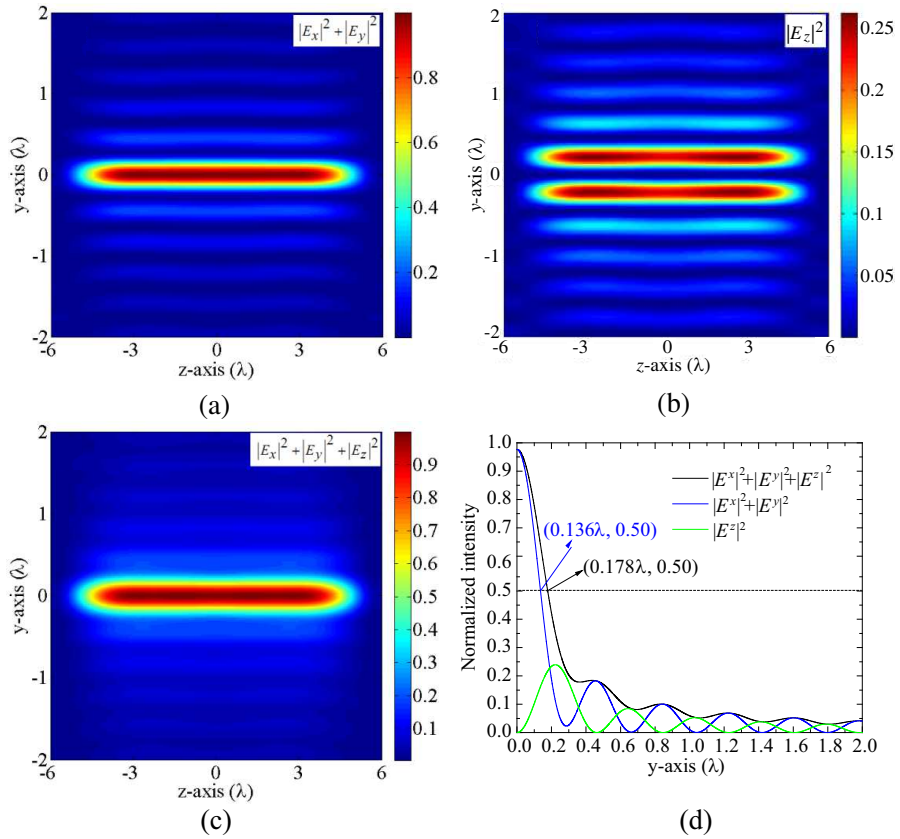


Figure 4. Electric energy density distributions on the y - z plane for the ternary optical element, (a) transverse component and (b) longitudinal component, (c) total electric energy density, (d) electric energy density component profile along the y -axis.

is $2 \mu\text{m}$, which is acceptable. The FWHM is 0.3573λ , and the DOF is 8.089λ , accordingly. One can find that the radii with three decimal digits can provide almost the same results as those with four decimal digits.

To further understand the optical characteristic of the super-resolution non-diffraction beam, Figure 4 shows the radial, longitudinal and total electric energy density distributions on the y - z plane.

Figure 4 shows that the transverse component [Figure 4(a)] occupies a dominant portion of the total electric energy [Figure 4(c)] and is localized. The longitudinal component [Figure 4(b)] is shaped

into a donut, which makes the spot size in the focal plane larger. The results on the characteristics of transverse and longitudinal components of the circularly polarized light are completely different from those of radially polarized light where the longitudinal component is localized and occupies most part of the total electric energy, and the parasitic radial component is donut-shaped. Figure 4(d) shows that the super-resolution non-diffraction beam has an FWHM of 0.3562λ , whereas that of the transverse component is 0.273λ , which means that the super-resolution effect is from the transverse component and that the longitudinal component increases the focal-spot size. The longitudinal component has been known to decay rapidly when it is inside the media, and thus the transverse component plays a dominant role in the spot size inside the media, thus the spot size of the super-resolution non-diffraction beam inside the media can theoretically reach down to 0.273λ . This property is very beneficial for optical data storage, optical coherent tomography, and three-dimensional confocal imaging and nanolithography because in these applications, the super-resolution non-diffraction beam needs to pass through the media.

Here it should be noted that the main differences between our work and that of [16] are as follows. Firstly, in [16], Wang et al. used radially polarized Bessel beam to generate the sub-wavelength non-diffraction beam, and the super-resolution effect was mainly from the contribution of longitudinal polarization component. In this work, the circularly polarized beam is chosen, and the super-resolution effect is from the transverse component. Secondly, Wang et al. just used binary phase-only plate to modulate the incident light, while in our work the combination of phase modulation with central block is adopted, and the super-resolution and DOF performances are better. Thirdly, the global searching optimization algorithm based on the confinement of the uniformity along the optical axis and FWHM in the focal plane is designed, which allows fast searching speed compared with traditional searching criteria.

4. CONCLUSION

In summary, we have proposed a fast searching method to design a ternary optical element combined with circularly polarized light to obtain super-resolution non-diffraction beam. The optimized results show that a beam with spot size of 0.356λ and DOF of 8.28λ can be obtained by using an oil lens with $NA = 1.4$ and refractive index of oil $n = 1.5$. Further analysis reveals that the transverse component of the super-resolution non-diffraction beam is 0.273λ , indicating that the super-resolution effect comes from the transverse component and

that the longitudinal component increases the spot size. The spot size inside the media can theoretically reach down to 0.273λ because the spot size of the super-resolution non-diffraction beam inside the media is mainly determined by the transverse component. The super-resolution non-diffraction beam is very useful for optical data storage, optical coherent tomography, and three-dimensional confocal imaging and nanolithography.

ACKNOWLEDGMENT

This work is partially supported by the National Natural Science Foundation of China (Grant Nos. 51172253, and 61137002), the Instrument Developing Project of the Chinese Academy of Sciences (Grant No. YZ201140), and the Science and Technology Commission of Shanghai Municipality (Grant Nos. 11JC1412700 and 11JC1413300).

REFERENCES

1. Grosjean, T., D. Courjon, and C. Bainier, "Smallest lithographic masks generated by optical focusing systems," *Opt. Lett.*, Vol. 32, 976–978, 2007.
2. Kim, W., N. Park, Y. Yoon, H. Choi, and Y. Park, "Investigation of near-field imaging characteristics of radial polarization for application to optical data storage," *Opt. Rev.*, Vol. 14, 236–242, 2007.
3. Quabis, S., R. Dorn, M. Eberler, O. Glockl, and G. Leuchs, "Focusing light to a tighter spot," *Opt. Commun.*, Vol. 179, 1–7, 2000.
4. Grosjean, T. and D. Courjon, "Smallest focal spots," *Opt. Commun.*, Vol. 272, 314–319, 2007.
5. Pazynin, L. A. and G. O. Kryvchikova, "Focusing properties of Maxwell's fish eye medium," *Progress In Electromagnetics Research*, Vol. 131, 425–440, 2012.
6. Dorn, R., S. Quabis, and G. Leuchs, "Sharper focus for radially polarized light beam," *Phys. Rev. Lett.*, Vol. 91, 233901, 2003.
7. Martinez-Corral, M., R. Martinez-Cuenca, I. Escobar, and G. Saavedra, "Reduction of focus size in tightly focused linearly polarized beams," *Appl. Phys. Lett.*, Vol. 85, 4319–4321, 2004.
8. Khonina, S. and I. Golub, "Optimization of focusing of linearly polarized light," *Opt. Lett.*, Vol. 36, 352–354, 2011.
9. Li, X., Y. Ye, and Y. Jin, "Impedance-mismatched hyperlens

- with increasing layer thicknesses,” *Progress In Electromagnetics Research*, Vol. 118, 273–286, 2011.
10. Liu, Z., H. Lee, Y. Xiong, C. Sun, and X. Zhang, “Far-field optical hyperlens magnifying sub-diffraction-limited objects,” *Science*, Vol. 315, 1686, 2007.
 11. Rogers, E. T. F., J. Lindberg, T. Roy, S. Savo, J. E. Chad, M. R. Dennis, and N. I. Zheludev, “A super-oscillatory lens optical microscope for subwavelength imaging,” *Nat. Materials*, Vol. 11, 432–435, 2012.
 12. Zhang, Y. and M. A. Fiddy, “Covered image of superlens,” *Progress In Electromagnetics Research*, Vol. 136, 225–238, 2013.
 13. Cao, P., X. Zhang, W.-J. Kong, L. Cheng, and H. Zhang, “Superresolution enhancement for the superlens with anti-reflection and phase control coating via surface plasmon modes of asymmetric structure,” *Progress In Electromagnetics Research*, Vol. 119, 191–206, 2011.
 14. Yan, W., J.-D. Xu, N.-J. Li, and W. Tan, “A novel fast near-field electromagnetic imaging method for full rotation problem,” *Progress In Electromagnetics Research*, Vol. 120, 387–401, 2011.
 15. Wang, H., L. Shi, G. Yuan, X. Miao, W. Tan, and T. Chong, “Subwavelength and super-resolution nondiffraction beam,” *Appl. Phys. Lett.*, Vol. 89, 171102, 2006.
 16. Wang, H., L. Shi, B. Lukyanchuk, C. Sheppard, and C. T. Chong, “Creation of a needle of longitudinally polarized light in vacuum using binary optics,” *Nat. Photonics*, Vol. 2, 501–505, 2008.
 17. Kuang, C., X. Hao, X. Liu, T. Wang, and Y. Ku, “Formation of sub-half-wavelength focal spot with ultra long depth of focus,” *Opt. Commun.*, Vol. 284, 1766–1769, 2011.
 18. Lerman, G. and U. Levy, “Effect of radial polarization and apodization on spot size under tight focusing conditions,” *Opt. Express*, Vol. 16, 4567–4581, 2008.
 19. Richards, B. and E. Wolf, “Electromagnetic diffraction in optical systems. II. Structure of the image field in an aplanatic system,” *Proc. R. Soc. London Ser. A*, Vol. 253, 358–379, 1959.